TRIUMF Experiment E614
Test Chamber Calibration Code

Maher Quraan
University of Alberta/TRIUMF
November 30, 1998

Contents

1 Introduction

Due to the high precision required in this experiment, an accurate calibration of the drift chamber (DC) is necessary. The data acquired in August 1997 with the seven DC test planes have been used to investigate a method that would allow us to obtain such a calibration. In addition, since these calibrations would have to be repeated at regular intervals throughout the lifetime of this experiment, it is necessary to "automate" this process so that the calibration code would run with the least amount of intervention. The aim here is to only turn on a flag corresponding to the kind of calibration required, after which the code would run independently until a calibration is obtained. A calibration file would be printed out once this process is completed.

The results obtained here are a first attempt, several more tests are required to further investigate our sensitivities to these calibrations and to quantify the uncertainties associated with them. The purpose of this document is to discuss the method used for this purpose rather than to present results.

The calibrations required for the DC include:

1. Drift distance as a function of time so that the time obtained from the TDCs may be converted into a drift distance and used in the tracking.
2. TDC time zero, which provides the zero reference point for the TDC data.
3. Finding the accurate positions (X or Y) for all planes in the DC.
4. Finding the accurate positions (X or Y and Z) for all wires in the DC.
5. Chamber resolution.

2 Drift Distance Calibrations

There are two methods to obtain a calibration for the drift distance as a function of TDC time:

1. Using the data itself to obtain this calibration by assuming that the integral of the TDC spectrum is proportional to the drift distance.
2. Using GARFIELD to obtain the calibration, which requires supplying GARFIELD with all the details about the chamber.

The assumption that the drift distance is proportional to the integral of the TDC spectrum follows from the following argument. For tracks traversing the cell at 0^0 the number of hits arriving from a strip of the cell of thickness dx is dN, such that

$$dN(x) = ndx, \tag{1}$$

where n is the number density of tracks across the cell (which is a constant if we assume the tracks are equally distributed through the cell). We then have

$$dN(t) = nv_d(t)dt, \tag{2}$$

where v_d is the drift velocity of the electrons. The quantity $dN(t)/dt$, therefore, corresponds to our TDC spectrum, where dt is the TDC channel width. The drift distance d(t) for electrons arriving from a distance with coordinates (t, x) at a wire with coordinates (t_w, x_w) is then given by

$$d(t) = \int_{t_w}^{t} v_d(t')dt' \propto \int_{t_w}^{t} \frac{dN(t')}{dt'}dt', \tag{3}$$

and is therefore proportional to the integral of the TDC spectrum, provided that n is a constant.

Since the field around the wires is not spherically symmetric, tracks traversing the detector at different angles will result in TDC spectra with different shapes. The drift distance $d(t)$ is therefore a function of the track angle as well as time, $d = d(t, \theta_t)$. If the data is used to obtain a drift distance calibration, it is necessary to bin the data in angle, with a bin size that is as fine as is required to obtain the desired resolution).

GARFIELD, on the other hand, generates a detailed mapping of the field inside the cell. Figure 1 shows a GARFIELD map of three drift cells at $1850V$. Figure 2 shows the drift distance as a function of TDC time as obtained from GARFIELD at the same high voltage and a 0^0 chamber orientation relative to the beam. While this provides a good starting point, a detailed understanding of GARFIELD is desired to improve on the accuracy of this calibration, including discriminator threshold effects and sensitivity to pressure, temperature, gas mixture and track angle. It is also worth noting that if the first calibration method is used (i.e. integrating the TDC spectrum instead of using GARFIELD), it may serve as a starting point, followed by several iterations (using tracking information) to fine-tune the calibration file. However, this iteration may also be done if we start with GARFIELD, with the added advantage that starting with GARFIELD will cut down on the number of iterations required.

We propose generating a 2-d matrix for the drift distance R_d as a function of the angle of the track θ_t and the (TDC) time t, $R_d(\theta_t, t)$, with a time bin width of 1 TDC channel ($0.5ns$) and a θ_t bin width comparable to our θ_t resolution ($\sim 0.5^o$, unless GARFIELD shows that we are less sensitive to angular variations).

3 TDC Time Zero

A determination of TDC time zero (T_0) is required for each TDC channel in the chamber. A first "guess" was made by estimating T_0 from the TDC spectrum of each plane. The TDC arrival time is shown in figure 3 for the five X planes. As may be seen from these figures the width of the rise time of the TDC spectra is 10-14 TDC channels (5-7ns). Choosing the midpoint of this range would therefore result in a limit error of 2.5-3.5ns. It was also found that the variation in T_0 from wire to wire in the same plane is negligible. However, T_0 is high voltage dependent so that a different calibration has to be obtained for runs at different high voltages.

Once an initial estimate of T_0 was obtained, an iteration was conducted to find a more

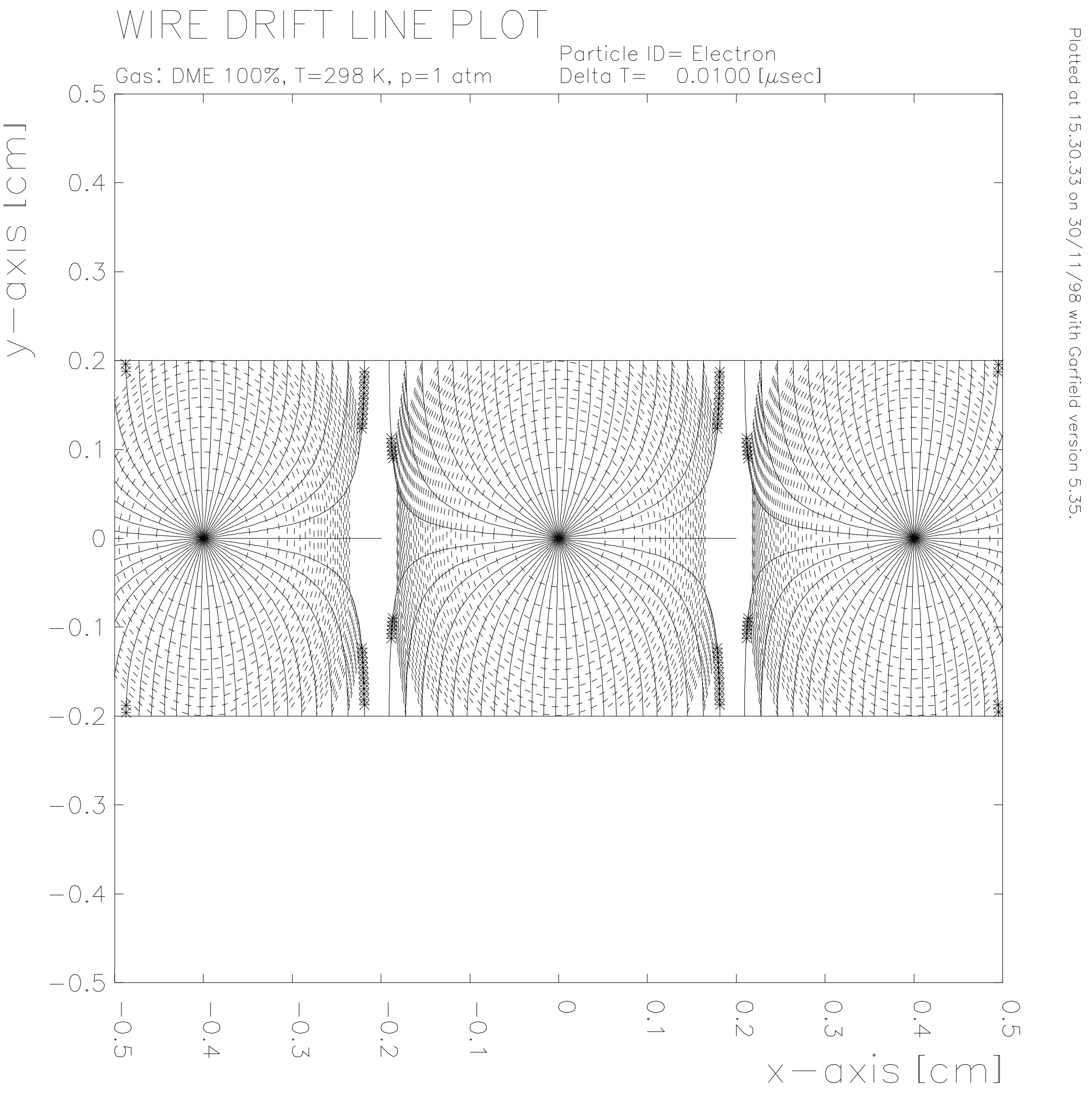

Figure 1: GARFIELD map of three drift cells for pure DME at 1850 V. The "radial" lines are electric field lines. The elipses are eqaul time contours spaced at $10ns$ intervals.

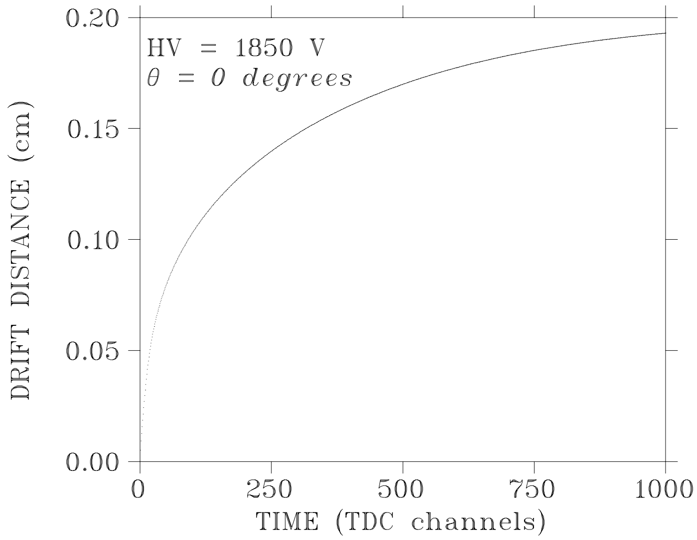

Figure 2: Drift distance as a function of TDC time as obtained from GARFIELD for the X planes at a high voltage of 1850 V.

accurate T_0 using tracking information. A tracking residual δd (defined as the distance of closest approach between the hit position and the track) was calculated. An average tracking residual δd_{ave} defined by

$$\delta d_{ave} = \frac{1}{N}\sum_{i=1}^{N} \delta d_i \tag{4}$$

was also calculated, where N is the total number of points used in the fit. For the purpose of finding T_0, the polarity of the tracking residuals was defined to be negative when the track passes inside a drift circle and positive when the track passes outside the drift circle. This was done to indicate the direction of the bias in T_0. For example, if T_0 is exactly right (and neglecting the influence of other factors) the track would have to be tangent to the drift circle. On the other hand, if T_0 was underestimated (overestimated), the track would pass inside (outside) the drift circle. This definition, therefore, provides information about the direction as well as the amount of bias in T_0. Using few trials a table was obtained to convert the value of the average residuals to time (δT_0) and T_0 was adjusted by the corresponding amount. This allowed the process to be automated. Once the corresponding flag is turned on, the code would run independently and print out the T_0 results to an output file when the process is completed.

Due to the shape of the GARFIELD file (see figure 2) T_0 is most sensitive to tracks

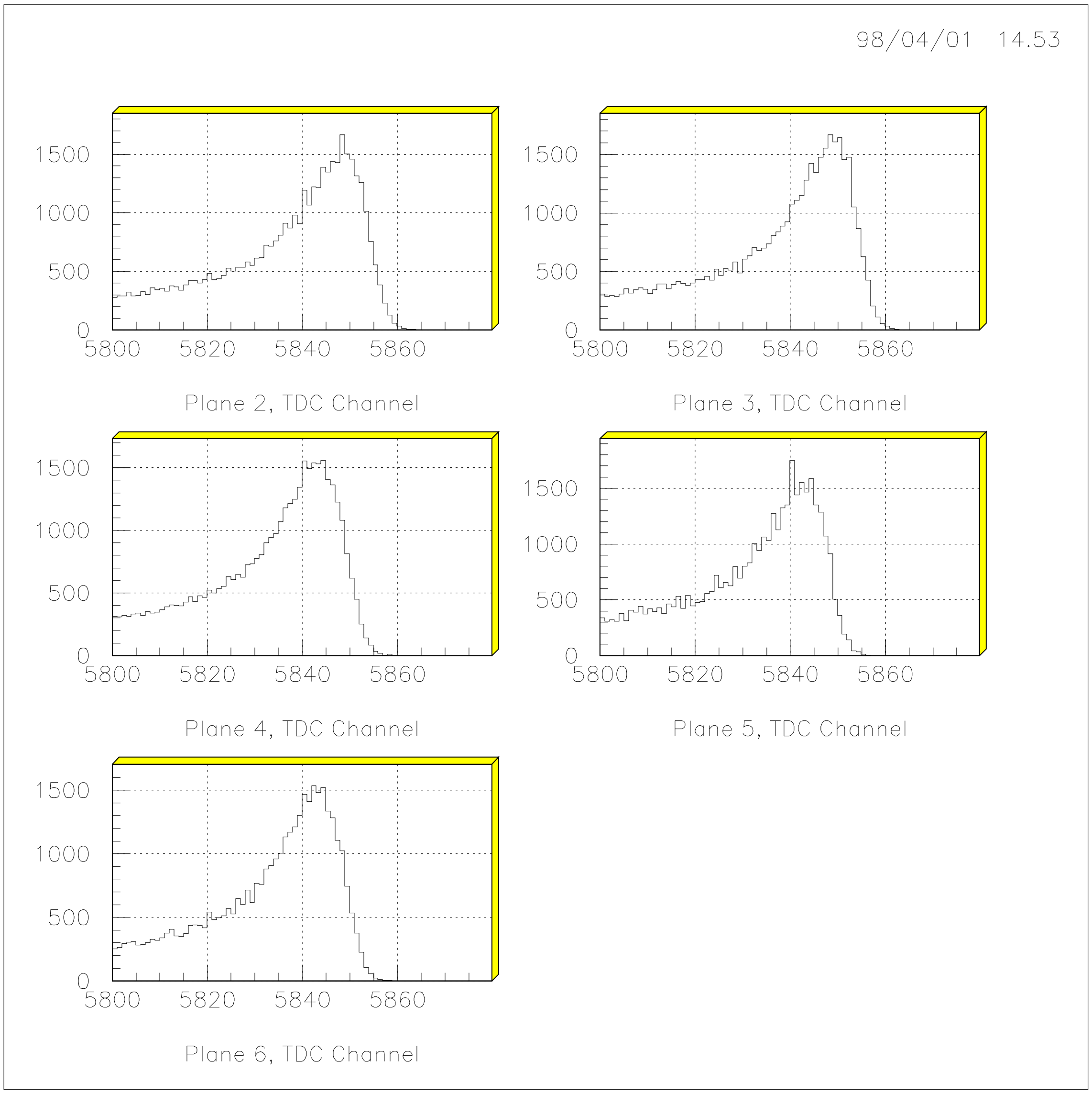

Figure 3: TDC spectra for the X planes from run 170 acquired at a high voltage of 1850 V with the new front end at a threshold of 140 mV.

passing close to the sense wire. To obtain T_0 only tracks passing within $500\mu m$ from the wire were used. This resulted in a shift of about $50\mu m$ corresponding to a shift of 1 TDC channel (note, however, that this is a rough estimate as the exact shift is highly dependent on the drift distance in this region being higher close to the wire). This implies that we should be able to find T_0 to within 1ns.

The following is a description of the algorithm:

1. Track N events.
2. Calculate the average tracking residual for each plane.
3. Translate the average residual to a T_0 shift (δT_0).
4. Adjust T_0 by δT_0.
5. Repeat the process until the average tracking residuals are within a specified amount from zero (i.e. until the process converges).

It is worth noting here that an iterative process is a must rather than a choice in obtaining this calibration. While T_0 is determined from tracking information, some initial T_0 has to be used as a starting point to calibrate the drift distance used in the tracking.

4 Plane Positions

The tracking is also useful in determining plane and wire positions. An iterative process is required here as well since the plane and wire positions are to be determined from the tracking but are also used to reconstruct the tracks. For this calibration the polarity of the tracking residuals was defined to be negative if the track passes to the left of a wire and positive if the track passes to the right of a wire. If the plane and wire positions are exactly where they should be (and ignoring other factors) the track would be tangent to the drift circle, and the average tracking residual would peak at zero. However, if the plane (or wire) is shifted to the left (right), the average tracking residual would be shifted to the right (left) by a corresponding amount. This information was then used to adjust the plane (wire) position by that amount.

It is worth noting here that when the polarity of the tracking residuals is defined to be negative (positive) when the track passes inside (outside) the drift circle, tracks passing to the left of a wire are mixed with tracks passing to the right of a wire. This serves an additional purpose, namely, sensitivity to wire (and plane) positions is minimized by averaging over left and right so that determination of T_0 is (to a reasonable extent) uncoupled from determination of wire positions. Similarly when the tracking residuals are defined to be negative (positive) if they pass to the left (right) of a wire, tracks passing inside a drift circle are mixed with tracks passing outside the drift circle so that sensitivity to T_0 is reduced.

The algorithm used for finding plane positions is as follows:

1. Track N events.
2. Calculate the average tracking residual for each plane.
3. Find the plane with the largest average residual (i.e. shift) and exclude it from the fit.
4. Track N events and compute new average residuals.
5. Shift the "removed" plane by its average residual.
6. Repeat the process until the average tracking residuals are within a specified amount from zero (i.e. until the process converges).

It was found that the X planes were shifted in x as follows:

plane	shift (μm)
2	0
3	17
4	117
5	-8
6	0

5 Wire Positions

The method used to find wire positions is analogous to that used to find plane positions. The algorithm used for this purpose is as follows:

1. Remove one plane from the fit for which the wire positions are to be determined.
2. Track N events.
3. Calculate the average tracking residual for each wire.
4. Shift each wire in the removed plane by its average residual.
5. Repeat the process until the average tracking residuals are within a specified amount from zero (i.e. until the process converges).

Figure 4 shows the wire positions obtained. As may be seen from this figure few wires are shifted by more than 10 microns. This is likely due to the limited number of iterations used in this test rather than a real wire misplacement. To confirm that an actual wire misplacement will be observed the position of one wire in each of the 5 X planes was assumed to be $\pm 100\mu m$ away from its actual position. The iteration process was then started. Figure 5 shows the position of each of the "shifted" wires at the end of each iteration. Only 32 iterations were done in this test. To speed up the convergence process a factor (F) was introduced so that the wires are "shifted" by $F * \delta d^w_{ave}$ (where δd^w_{ave} is the average tracking residual for that wire). In figure 6 the factor F was chosen to be 3. Only 16 iterations were done in this case. It is not clear at this point why the shifted wire in plane 6 did not converge as fast as the wires in the other 4 planes. It should be emphasized again, however, that these tests were exploratory. Further testing is still required to fully understand this process.

6 Chamber Resolution

Figure 7 shows a histogram of the tracking residuals, δd, and the average tracking residuals, δd_{ave}, obtained from the fit for data acquired at 1850 V and a chamber orientation of 0^o. The width of the tracking residuals reflect the intrinsic resolution of the chamber as well as all other factors that may contribute to inaccuracies in the tracking. This includes wire positions, drift distance (where both uncertainties in T_0 and the GARFIELD calibration file contribute). In addition, it reflects any biases in the fitting process, as well as the weighting used in the fit. The reasonably narrow width obtained and the level of symmetry of this histogram provides reasonable confidence in all these factors.

The tracking resolution of the chamber may be determined from the width of the tracking residuals. However, the resolution has a strong dependence on drift distance. The widths of the tracking residuals were determined in 10 bins across the cell (200 μm wide). Since the tracking residuals themselves are dependent on the accuracy of the fit and, therefore, on the weighting of the fit (which is in turn dependent on what we assume the chamber resolution is as a function of the drift radius), an iterative process is required. After each turn in this iteration, the widths of the 10 tracking residual histograms were determined, fitted to an eight-parameter polynomial and the results were used to weight the fit. A total of 22 iterations were required for this process to converge, after which the resolutions were changing by $< 0.1 \mu m$. Figure 8 shows the result. The chamber resolution improves as a function of drift radius due to the increase in ionization statistics. This general result is independent of gas type, although DME provides high ionization compared to other gases and, therefore, both a more steep increase in the resolution as a function of drift radius and a higher overall resolution. While our result is generally consistent with other experiments the minimum resolution obtained (which occurs near $0.15 \mu m$) is

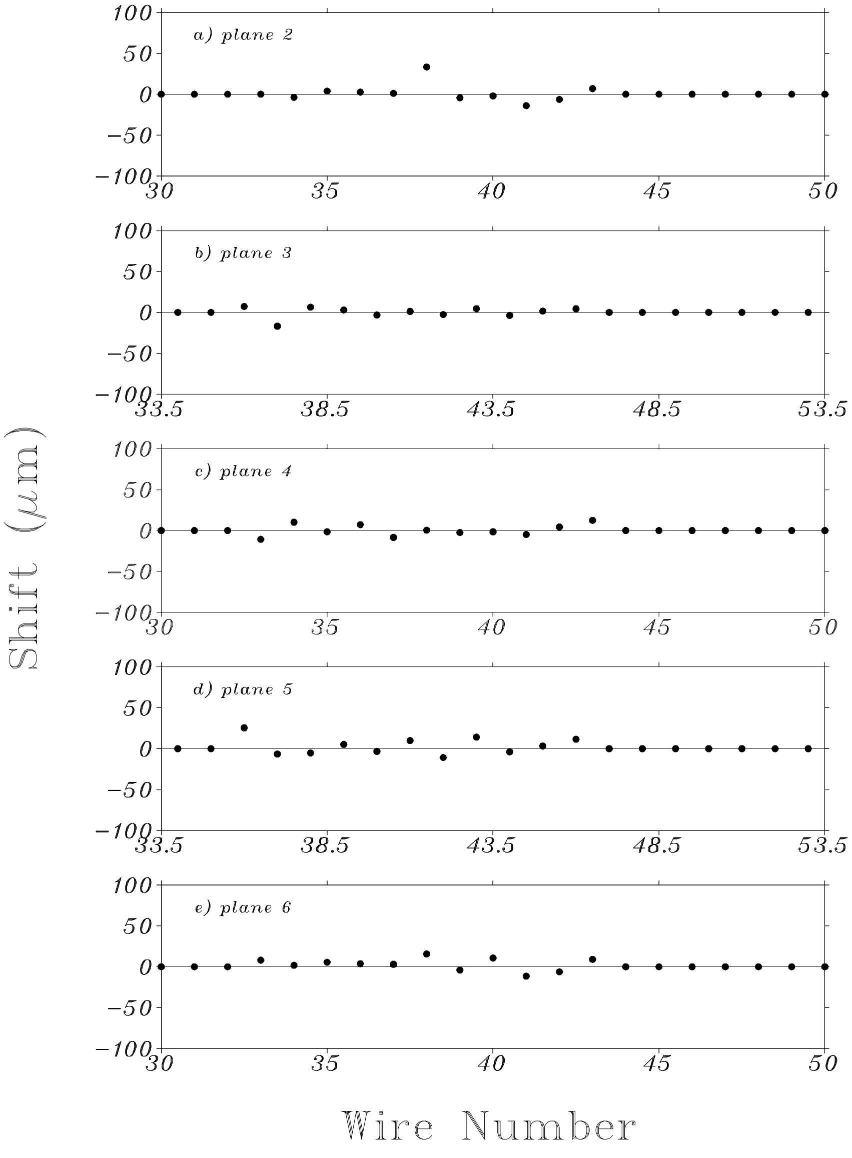

Figure 4: Wire displacement for the 5 X planes used in the DC prototype test in August 1997.

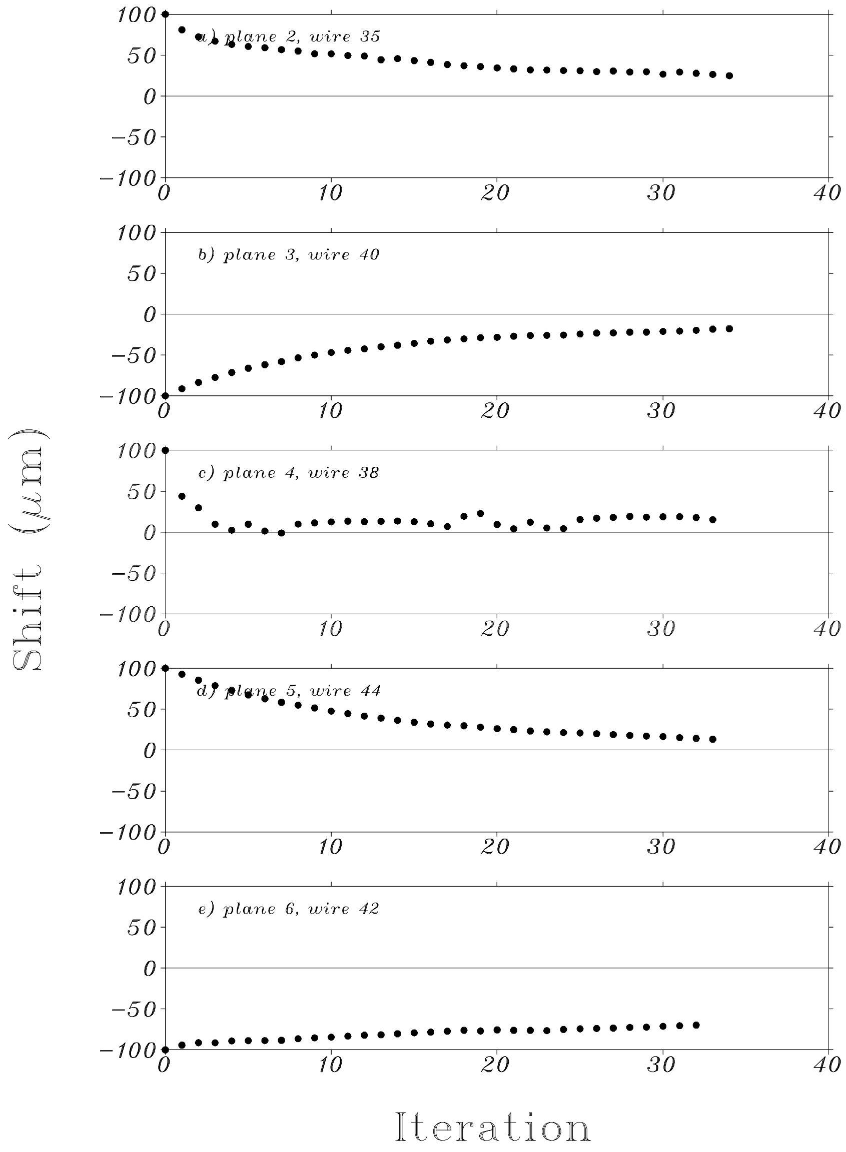

Figure 5: Wire displacement after each iteration for each of the shifted wires for F=1 (see text above).

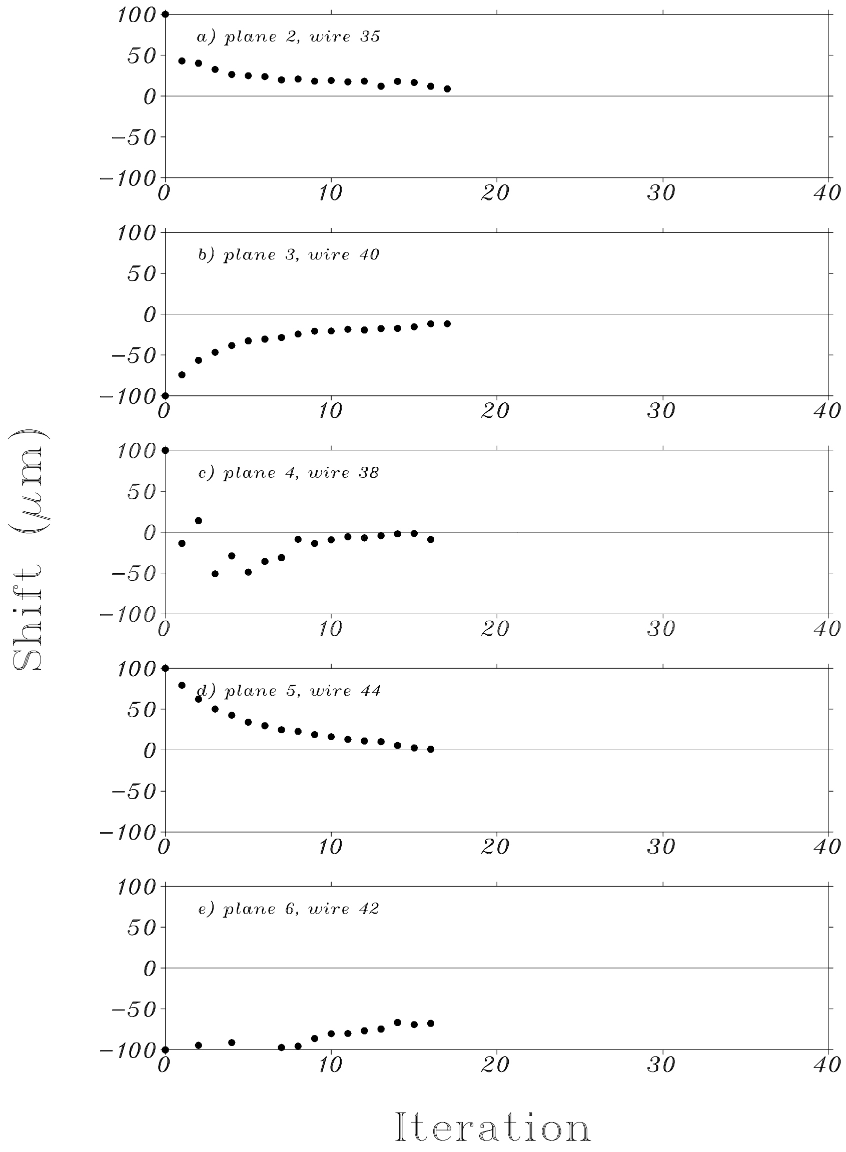

Figure 6: Wire displacement after each iteration for each of the shifted wires for F=3 (see text above).

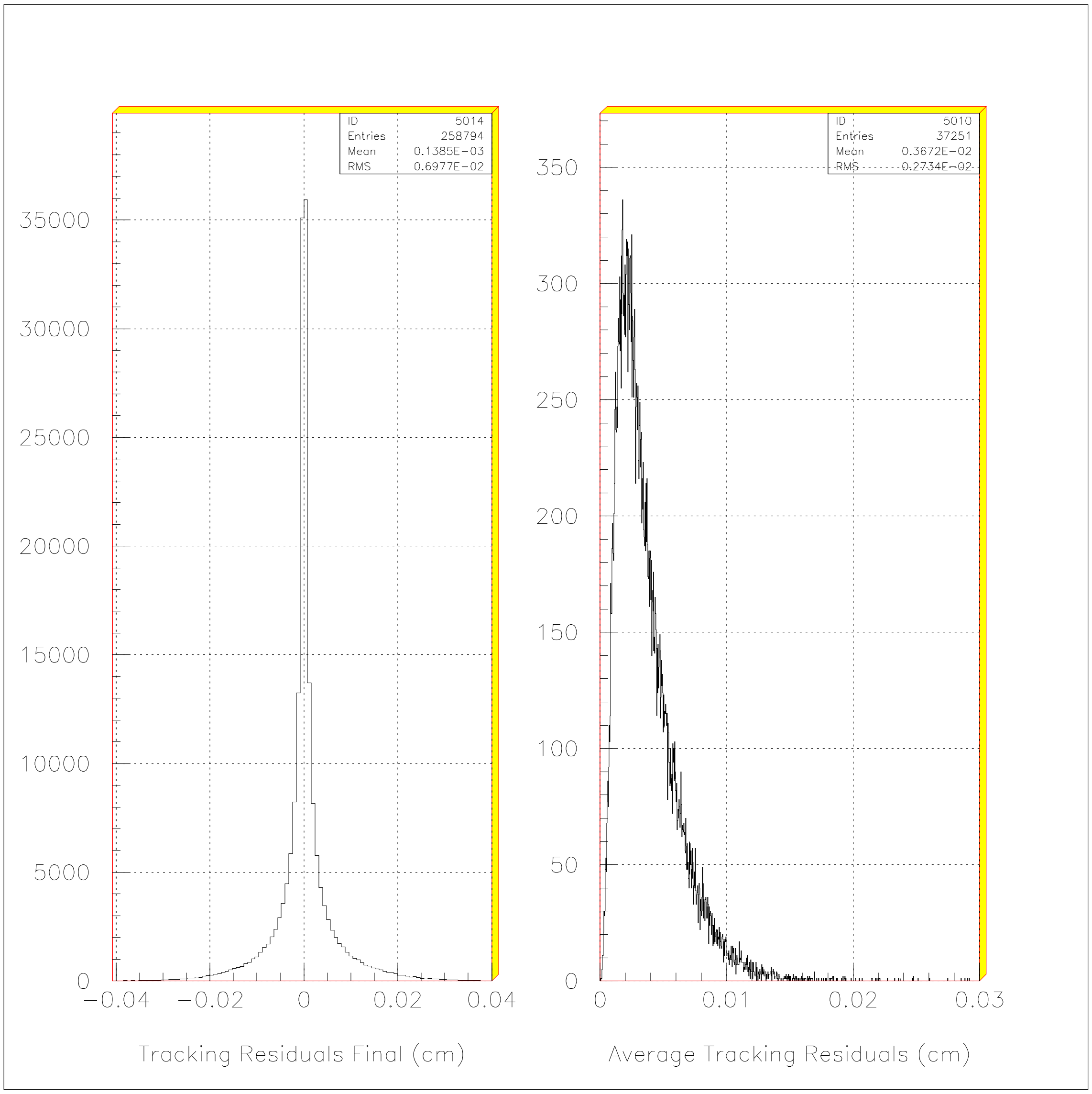

Figure 7: Tracking residuals (for each hit) and average tracking residuals (per event) for data acquired at a high voltage of $1850V$ and a chamber orientation of 0^o.

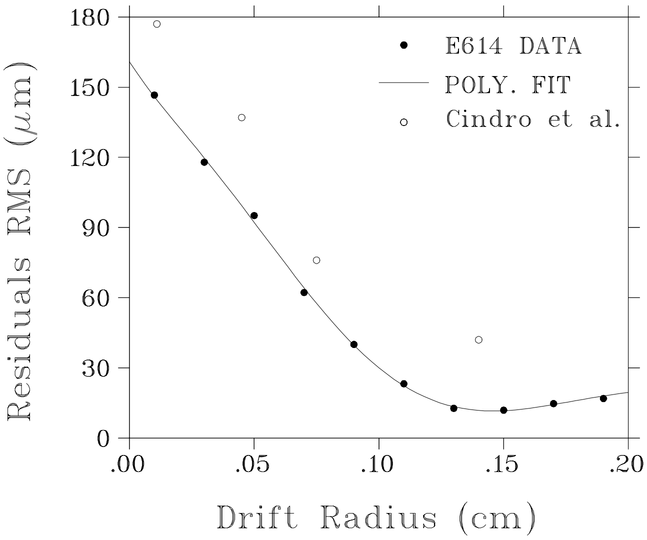

Figure 8: Chamber resolution as a function of drift radius. The dots are computed from data acquired at 1850 V and a chamber orientation of 0^0; the curve is an eight-parameter polynomial fit to the data. The circles are data from Cindro et al. obtained with a drift chamber that has a cell size of 10.4 mm $\times$ 11.4 mm and filled with pure DME gas.

about $12\mu m$ in our experiment compared to $30\mu m$ for the other experiments. However, as mentioned above, the widths of the tracking residuals (from which these resolutions are determined) reflect on the accuracy of the calibrations, tracking method etc., all of which might have contributed to the lower resolutions obtained in these other experiments (for example inaccuracies in wire positions would smear out the total residuals).

In the calcultaion above the resolution of all the DC planes was calculated simeltaneously assuming no plane-to-plane variations. Variations in gas mixture or high voltage from plane to plane would cause the resolution to be plane dependent. The apparent resolution of one plane may also be different if an inappropriate choice of TDC0 for that plane was made, or inaccurate wire positions were used. It might prove useful to calculate the resolution on a plane-by-plane basis (at least for the purpose of testing).

Since this calculation was made, the resolution calculation was automated so that the iteration will proceed once the proper flag is turned on until the process converges. At the end of this process the parameters of the fit will be printed to an output file.

7 Conclusions

The tests done so far to calibrate the 5 X DC planes that were used in August 1997 have shown that an accurate calibration of the DC is possible. Further testing is still required to understand this process and modify the existing code accordingly. Although all the calibrations discussed above were done using tracking residual information, the proper choice of the definition of the tracking residuals helps minimize their interdependence. The effect of one calibration on another, however, may not be completely eliminated. Some overall iteration will, therefore, be required.

The calibration process of the entire DC will prove to be time consuming and cpu demanding. Perhaps the best way of dealing with this is to assign the task to one person/institution to be responsible for obtaining the calibration files and maintaining the Calibration File Manager (CFM) for the data analysis. A dedicated computer may have to be provided for the job.